



# Transient and intermediate carbocations in ruthenium tetroxide oxidation of saturated rings

Manuel Pedrón<sup>1</sup>, Laura Legnani<sup>2</sup>, Maria-Assunta Chiacchio<sup>2</sup>, Pierluigi Caramella<sup>3</sup>, Tomás Tejero<sup>4</sup> and Pedro Merino<sup>\*1</sup>

## Full Research Paper

Open Access

### Address:

<sup>1</sup>Instituto de Biocomputación y Física de Sistemas Complejos (BIFI), Campus San Francisco, Universidad de Zaragoza, 50009 Zaragoza, Spain, <sup>2</sup>Dipartimento di Scienze del Farmaco, University of Catania, V.le A. Doria 6, 95125 Catania, Italy, <sup>3</sup>Dipartimento di Chimica, Università di Pavia, Via Taramelli, 12, 27100, Pavia, Italy and <sup>4</sup>Instituto de Síntesis Química y Catálisis Homogénea (ISQCH), Campus San Francisco, Universidad de Zaragoza-CSIC, 50009 Zaragoza, Spain

### Email:

Pedro Merino\* - pmerino@unizar.es

\* Corresponding author

### Keywords:

alkanes; carbocations; DFT; oxidations; ruthenium tetroxide

*Beilstein J. Org. Chem.* **2019**, *15*, 1552–1562.

doi:10.3762/bjoc.15.158

Received: 02 March 2019

Accepted: 02 July 2019

Published: 11 July 2019

This article is part of the thematic issue "Reactive intermediates – carbocations".

Guest Editor: S. R. Hare

© 2019 Pedrón et al.; licensee Beilstein-Institut.

License and terms: see end of document.

## Abstract

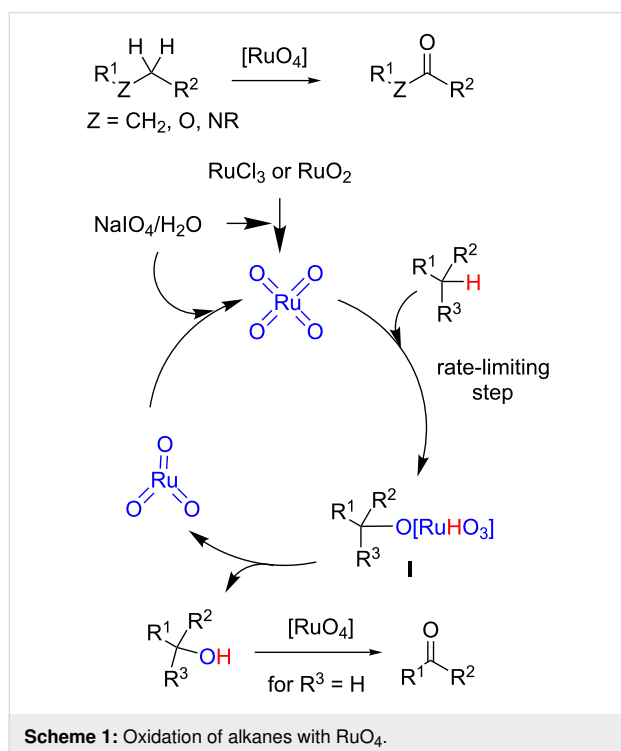
The ruthenium tetroxide-mediated oxidation of cyclopentane, tetrahydrofuran, tetrahydrothiophene and *N*-substituted pyrrolidines has been studied computationally by DFT and topological (analysis of the electron localization function, ELF) methods. In agreement with experimental observations and previous DFT calculations, the rate-limiting step of the reaction takes place through a highly asynchronous (3 + 2) concerted cycloaddition through a single transition structure (one kinetic step). The ELF analysis identifies the reaction as a typical one-step-two-stages process and corroborates the existence of a transient carbocation. In the case of pyrrolidines, the carbocation is completely stabilized as an energy minimum in the form of an iminium ion and the reaction takes place in two steps.

## Introduction

Ruthenium-catalyzed oxidations [1,2] and, in particular, those involving ruthenium tetroxide [3,4] occupy a privileged position among the modern oxidation methods due to their versatility regarding functional groups that can be oxidized and formed [5]. Alkane functionalization continues to be a current challenge in organic synthesis [6] and oxidation with rutheni-

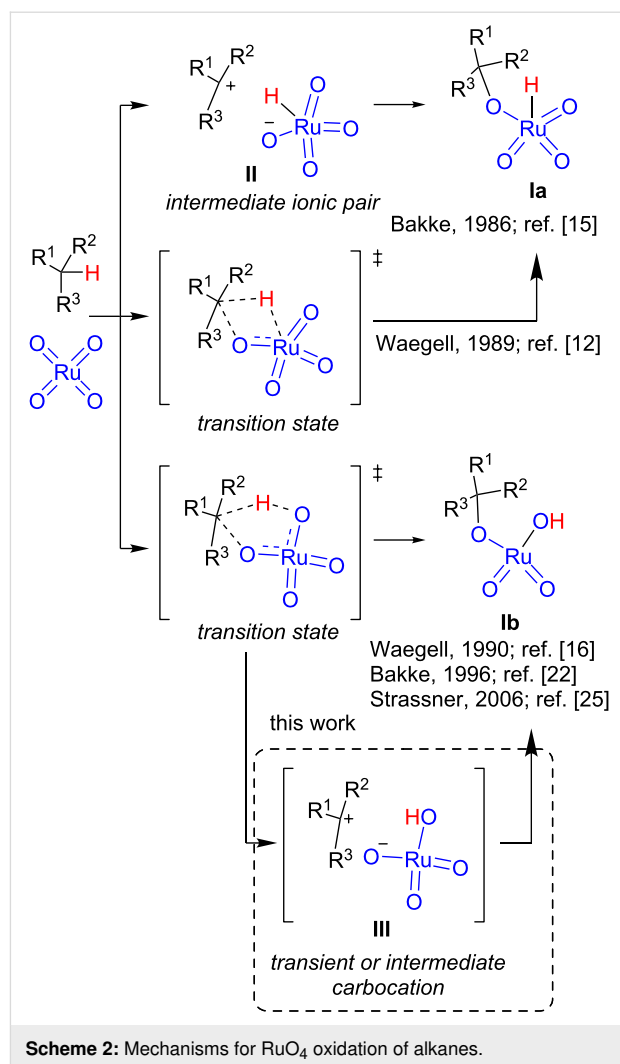
um tetroxide allows to introduce an oxygenated functionality (alcohol or carbonyl) into a saturated carbon skeleton [7]. Moreover, if oxygen or nitrogen atoms are present, the reaction leads to the formation of esters [8,9] or amides [10,11], respectively (Scheme 1). The reaction is typically performed by preparing ruthenium tetroxide in situ from ruthenium species in

lower oxidation states ( $\text{RuCl}_3$  or  $\text{RuO}_2$ ) and an oxidant such as  $\text{NaIO}_4$  [8]. Under these conditions  $\text{RuO}_4$  reacts with the alkane to form intermediate species **I** that evolves to the alcohol and  $\text{RuO}_3$ , which is re-oxidized to re-start the catalytic cycle (Scheme 1) [12]. Depending on the substrates and reaction conditions (re-oxidant, solvent, temperature) the alcohol can be oxidized to the corresponding carbonyl derivative [13,14].



The rate-limiting step of the catalytic cycle illustrated in Scheme 1 is the initial reaction between  $\text{RuO}_4$  and the alkane, and it has been studied both experimentally and computationally having some initial controversy. The first studies were reported by Bakke et al. in 1986 who suggested the formation of intermediate ionic species on the basis of kinetic isotopic effects and solvent and substituents effects (Scheme 2) [15]. Three years later, Waegell et al. proposed a (2 + 2) concerted mechanism [12], although the intimate nature of the organometallic intermediates was not completely elucidated [16]. After some discussion in which Bakke et al. confirmed their initial proposal [17,18] and Waegell et al. proposed a new (3 + 2) asynchronous concerted mechanism [19,20], both groups converged to the latter proposed mechanism when Bakke et al. changed the interpretation of their kinetic isotopic experiments [21–24].

The (3 + 2) concerted mechanism was further confirmed by DFT calculations [25] which were also in agreement with the earlier experiments of Bakke et al. [15]. The computational study also confirmed the hydroxide adduct **Ib** as the active

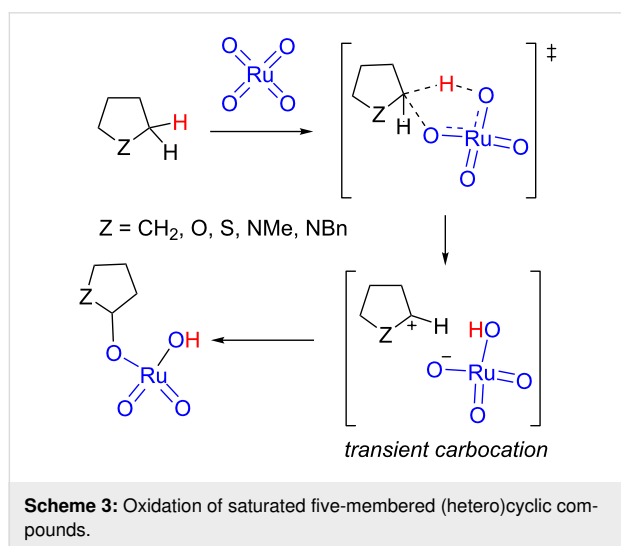


intermediate formed in the reaction. However, Petride et al. have demonstrated that iminium cations are intermediates in the  $\text{RuO}_4$ -mediated oxidation of tertiary amines [26] by trapping them with cyanide anion [27,28]. These results point out the formation of transient carbocations **III** that can be stabilized by the presence of heteroatoms in the alpha position. The formation of transient carbocations do not contradict, necessarily, the proposed asynchronous concerted mechanism. A deeper analysis of the full path of the reaction using MD calculations [29] would be needed in order to assess the synchronicity and life time of transient species [30]. The recent use of MD simulations has demonstrated that a single transition state can lead to different products in a ratio that depends on reaction dynamics [31–33]. The study of molecular dynamics trajectories has allowed characterization of ambimodal transition states in reactions involving carbocations [34,35].

We have demonstrated computationally the presence of transient carbocations in reactions taking place in one kinetic step

including asynchronous concerted cycloadditions [36] and  $\text{S}_{\text{N}}2$ -type reactions [37]. Moreover, the real existence of transient carbocations – which are not energy minima – predicted computationally has also been recently proven experimentally in a reaction with an only transition state in which a planar transient species is developed during the reaction [38]. The formation of transient carbocations developed along the reaction course cannot be detected by the calculation of stationary points alone. The use of topological methods, in particular the analysis of the electron localization function (ELF) [39,40] is an excellent approach to evaluate the synchronicity of organic reactions [41,42] and consequently, to predict the formation of transient carbocations [43].

In this work, we report a computational study of the  $\text{RuO}_4$ -mediated oxidation of cyclopentane, tetrahydrofuran, tetrahydrothiophene, and *N*-methyl- and *N*-benzylpyrrolidine to evaluate the extension in which transient carbocations can be formed (and whether they can become energy minima) during the rate-limiting step (Scheme 3). The  $\text{RuO}_4$  oxidation of cyclopentane [44] and tetrahydrofuran [45] have been experimentally reported as well as the oxidation of *N*-acylpyrrolidines to the corresponding lactams [46]. Admittedly, the oxidation of tetrahydrothiophene has been approached only computationally since in that case the sulfur atom would be more easily oxidized. Since the general mechanism consisting of a (3 + 2) transition state has been confirmed as the preferred one [25], we restricted the study to this approach.



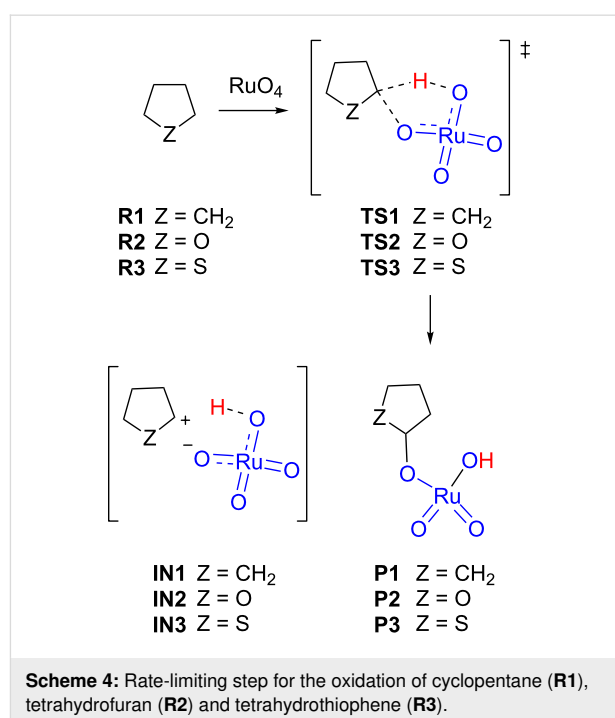
## Computational Methods

The procedures are analogous to those previously reported [43]. All of the calculations were performed using the Gaussian 09 program [47]. Computations were done using the B3LYP functional [48,49] in conjunction with Grimme's dispersion correc-

tion [50,51] (henceforth referred to as B3LYP-d3bj). The standard basis set Def2SVP was employed [52,53]. For the purpose of comparison optimizations at gas phase and considering solvent effects (both acetonitrile and water, CPCM [54,55]) were carried out. The optimizations were carried out using the Berny analytical gradient optimization method [56]. Minimum energy pathways for the reactions studied were found by the corresponding IRC analysis [57], using the Hratchian–Schlegel algorithm [58]. The individual reactions involved in the study are bimolecular processes. In order to avoid errors due to entropic effects when comparing all stationary points in an only energy diagram, a correction to free energy was made by subtracting Strans contribution and considering a 1 M concentration [59]. Single point calculations at the  $3\xi$  level of theory, using the Def2TZVP basis set and considering solvent effects, were carried out over optimized geometries to obtain more accurate energy values. The electronic structures of stationary points were analyzed by the topological analysis of the gradient field of electron localization function (ELF) [39,40,60–66]. The ELF study was performed with the TopMod program [67] using the corresponding monodeterminantal wavefunctions of all the structures of the IRC. Structural representations were generated using CYLView [68]. The models used for calculations are those indicated in Scheme 3.

## Results and Discussion

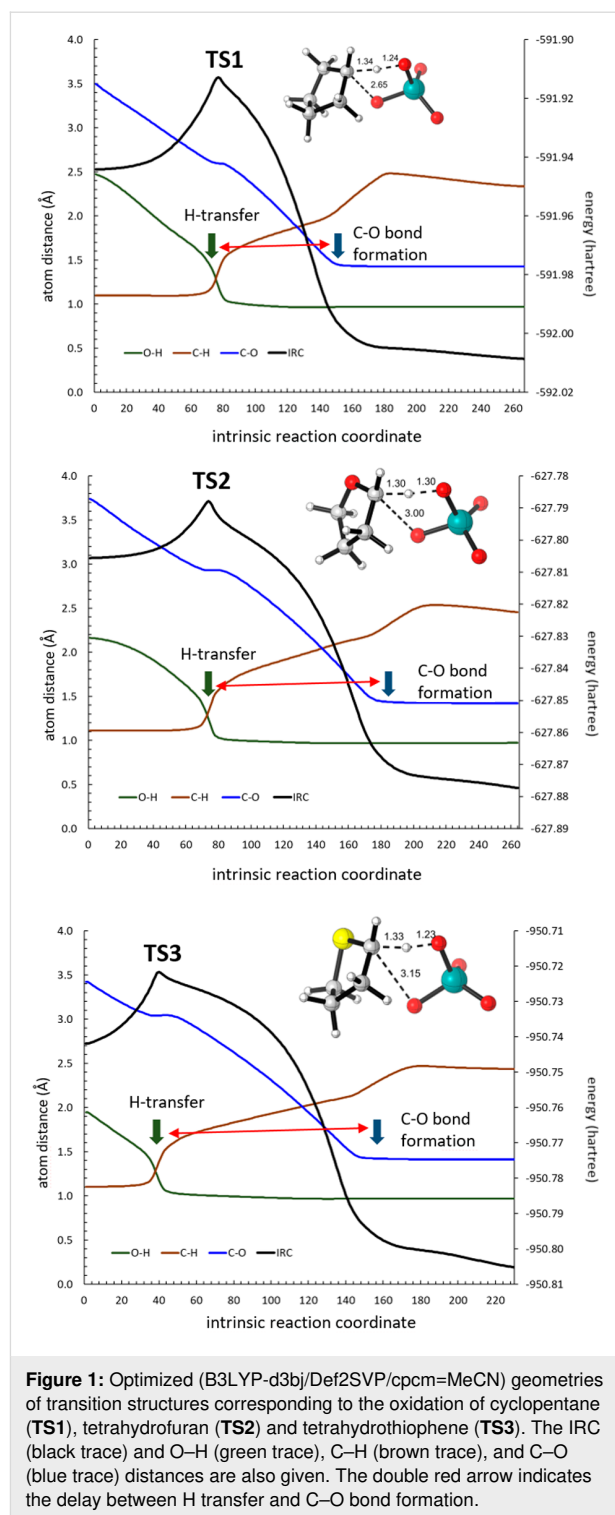
We first studied the oxidations of cyclopentane (**R1**), tetrahydrofuran (**R2**) and tetrahydrothiophene (**R3**, Scheme 4). The geometries of all stationary points were optimized at the



B3LYP-d3bj/Def2SVP level of theory in the gas phase and considering solvent effects for acetonitrile and water and their corresponding energy values were calculated at the same level. Since the experimental conditions for the oxidation reactions usually involve a polar medium containing water, all discussions were based on data obtained considering solvent effects for water (for the results using other levels of theory see Supporting Information File 1). We located the corresponding transition structures **TS1**, **TS2** and **TS3**. Any attempt to locate (and optimize) ionic pairs **IN1**, **IN2** and **IN3** failed and, in all cases, the optimization ends at the corresponding products **P1–3**, clearly indicating that those ionic pairs are not stable as energy minima even in highly polar conditions (modelled using continuum water solvent).

The obtained energy barriers were 14.6, 6.0 and 7.5 kcal/mol for **TS1**, **TS2** and **TS3**, respectively, predicting an easier oxidation for the heterocyclic compounds. Similar differences between the barriers were obtained in acetonitrile (barriers of 16.6, 8.0 and 8.8 kcal/mol for **TS1**, **TS2** and **TS3**, respectively); the highest observed barriers with respect to water are in agreement with a highly polar reaction.

The corresponding transition structure for cyclopentane **TS1** showed a typical geometry for an asynchronous concerted reaction (Figure 1) in agreement with that observed in the previous study carried out at the B3LYP/6-31G(d) level of theory with implicit MeCN solvent [25]. In that study, the forming/breaking bond distances (estimated for decalines in acetonitrile and acetone) were in the following ranges: the C–H bonds were 1.37–1.41 Å, the O–H bonds were 1.19–1.22 Å, and the C–O bonds were 2.57–2.84 Å. The observed values for **TS1** in water (C–H: 1.34 Å; O–H: 1.24 Å and C–O: 2.65 Å) and acetonitrile (C–H: 1.34 Å; O–H: 1.24 Å and C–O: 2.64 Å) were similar, but placing the hydrogen atom slightly closer to the carbon atom. Similar distances for the C–H–O system were found for **TS2** (C–H: 1.30 Å and O–H: 1.30 Å) and **TS3** (C–H: 1.33 Å and O–H: 1.23 Å), corresponding to tetrahydrofuran and tetrahydrothiophene, respectively. On the other hand, the C–O distance increased to 3.00 Å in **TS2** and to 3.15 Å in **TS3** (similar data were found in acetonitrile, see Supporting Information File 1) clearly indicating a delay in the formation of the C–O bond. This situation is compatible with the stabilization of a developing positive charge at the carbon atom by a mesomeric effect of the  $\alpha$ -heteroatom. Nevertheless, the corresponding IRCs for the three transition structures confirmed a concerted reaction connecting the corresponding encounter pairs **EP1**, **EP2** and **EP3** (see Supporting Information File 1), formed from reagents **R1–3** and ruthenium(IV) tetroxide, with **P1**, **P2** and **P3**, respectively. A close inspection of the IRCs revealed a shoulder characteristic of a transient carbocation [23] which is



more pronounced following the sequence **R1** < **R2** < **R3**. The preliminary analysis of the evolution of bonds along those IRCs further confirmed a high asynchronicity, showing a substantial delay in the formation of the C–O bond with respect to the H transfer from the C atom to the O atom, and following the sequence **TS1** < **TS2** < **TS3** (Figure 1, red arrows).

Even though the above data clearly point out to a typical one-step-two-stage process [69–71] in which the bonds are broken and formed in two separate events, only a topological analysis of the ELF will provide the exact moment in which those events take place and provide evidences of the formation of a transient carbocation. The ELF analysis [39,40,72,73] allows calculation of the so-called basins of attractors [74], that are the areas in which the probability of finding an electron pair is maximal. Monosynaptic and disynaptic basins correspond to separate atoms and bonds, respectively. When a bond is formed, two monosynaptic basins merge into a new disynaptic basin.

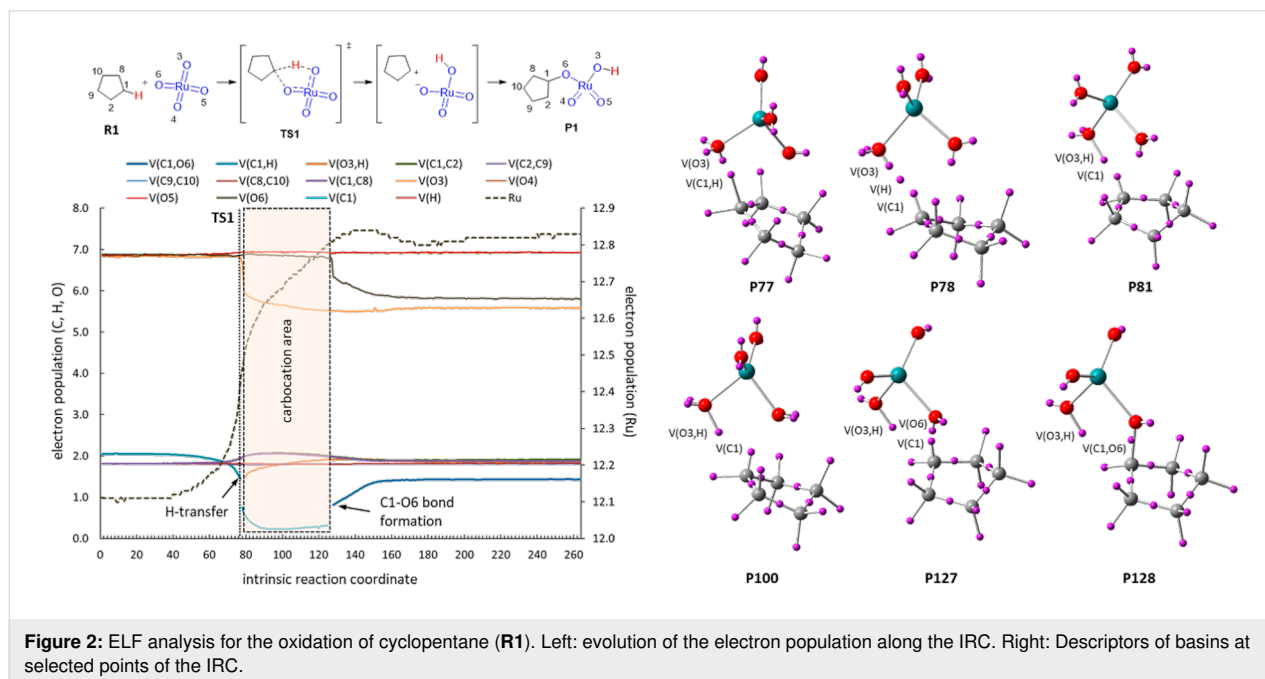
The complete ELF analyses of the IRCs corresponding to **TS1**, **TS2** and **TS3** have allowed identifying changes in the electron distribution of atoms and bonds during the reaction coordinate and the precise moment in which bonds are broken and formed.

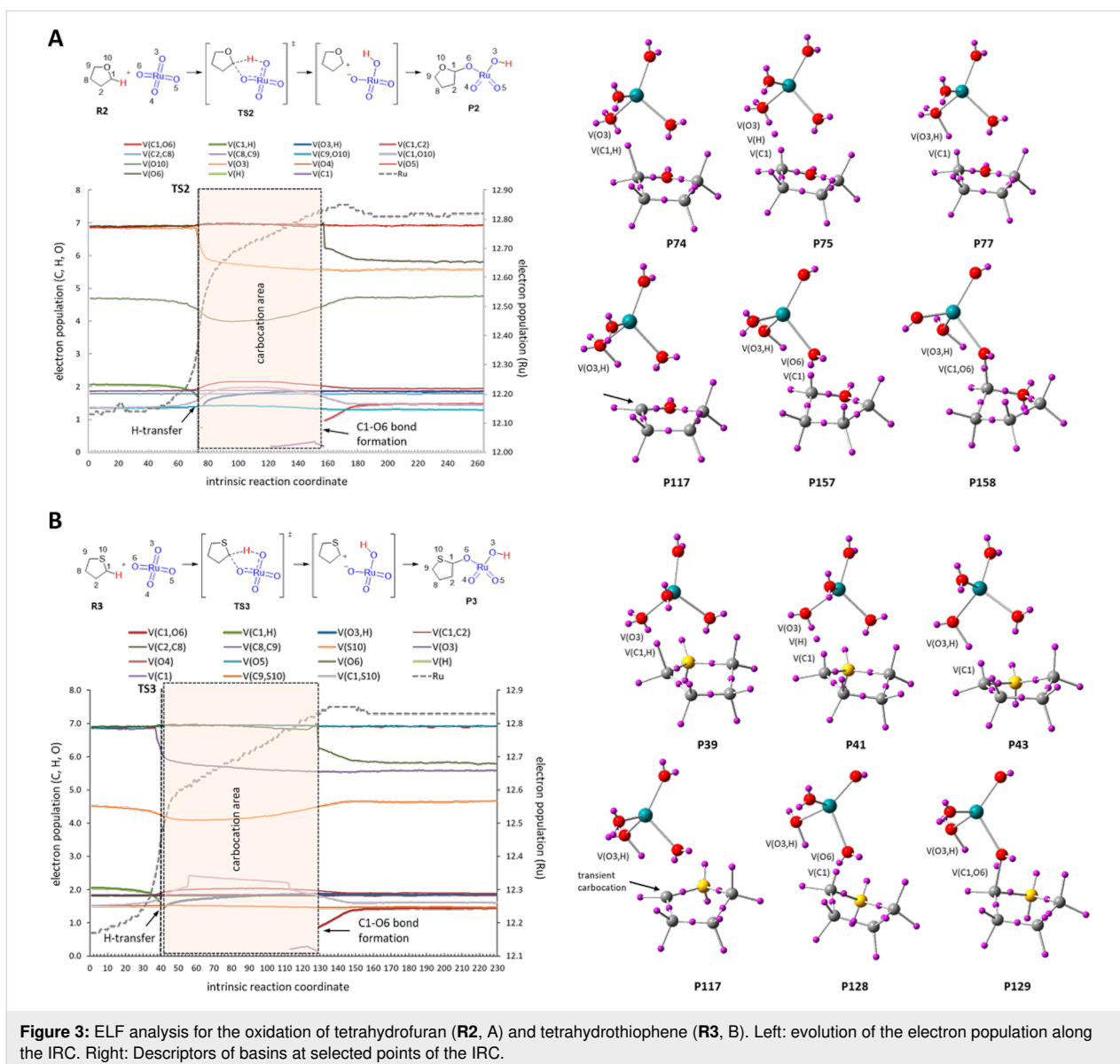
The ELF analysis of the oxidation of cyclopentane (Figure 2) showed an asynchronous concerted process with the transition state at point 77 (29% of IRC). Breaking of the C1–H bond is immediately followed by H transfer (point 78) and O3–H bond formation (point 81). The formation of the second C–O bond takes place at point 128 (48% of IRC). The gap between H transfer and C1–O6 bond formation (from point 81 to point 127, corresponding to 17% of IRC) is compatible with the existence of a transient carbocation at C1. Nevertheless, the reaction might also be considered just an asynchronous concerted process with a clear partial charge development during the formation of O3–H and C1–O6 bonds that takes place in two separate events.

The stabilization of the above-mentioned transient carbocation can be achieved by introducing heteroatoms. The ELF analysis corresponding to the oxidation of tetrahydrofuran (Figure 3A) again showed a typical one-step-two-stage situation. In this case, the gap between the H transfer and the formation of C1–O6 bond (from point 77 to point 157, corresponding to a 30% of the IRC) is larger than that of cyclopentane (corresponding to a 17% of IRC) as a consequence of the stabilizing effect of the incipient positive charge exerted by the oxygen atom. The effective existence of a transient carbocation is supported by the disappearance of V(C1) and the trigonal planar geometry observed for C1 in the above indicated gap. The evolution of the electron population is in clear agreement with the development of a partial positive charge at C1 (+0.25 at point 100). The oxidation of tetrahydrothiophene reflects the same situation, but to a greater degree (Figure 3B).

Interestingly, the ELF analyses evidence the high polarity of Ru–O bonds by assigning about 7e to the oxygen atoms. Because of this, during the reaction coordinate an increase of only 1e is assigned to Ru for which about 12e (coming from 4e of valence directly assigned plus 8e from the last layer  $4s^2 4p^6$ ) have been initially assigned (Figure 4). Although this assignment does not correlate with the classical valence concept of 8e for Ru(VIII) it actually reflects a more real situation.

As stated above, attempts of locating the corresponding ion pairs failed, ending at the final **P1–3** products and confirming that they are not stationary points. However, this does not mean



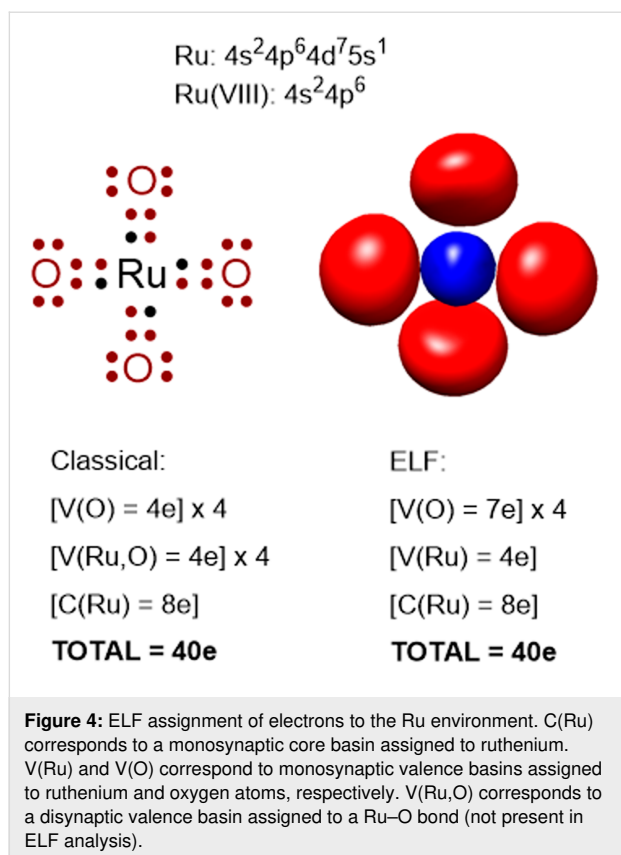


that they cannot exist in the form of transient species as we have recently demonstrated [38].

A completely different situation was found with the oxidation of *N*-methylpyrrolidine (**R4**) and *N*-benzylpyrrolidine **R5** (Scheme 5). In the case of *N*-alkylpyrrolidines two regioisomeric oxidations can take place at *endo* (cycle) and *exo* (*N*-chain) positions. We located the four transition structures **TS4a** and **TS5a**, corresponding to the *endo* series, and **TS4b** and **TS5b**, corresponding to the *exo* series.

In all cases, the observed barriers were below the reagents illustrating a favorable reaction (see Figure 5). For *N*-methylpyrrolidine (**R4**), the *endo* oxidation was preferred over the *exo* oxidation by 1.3 kcal/mol whereas for *N*-benzylpyrrolidine **R5** the

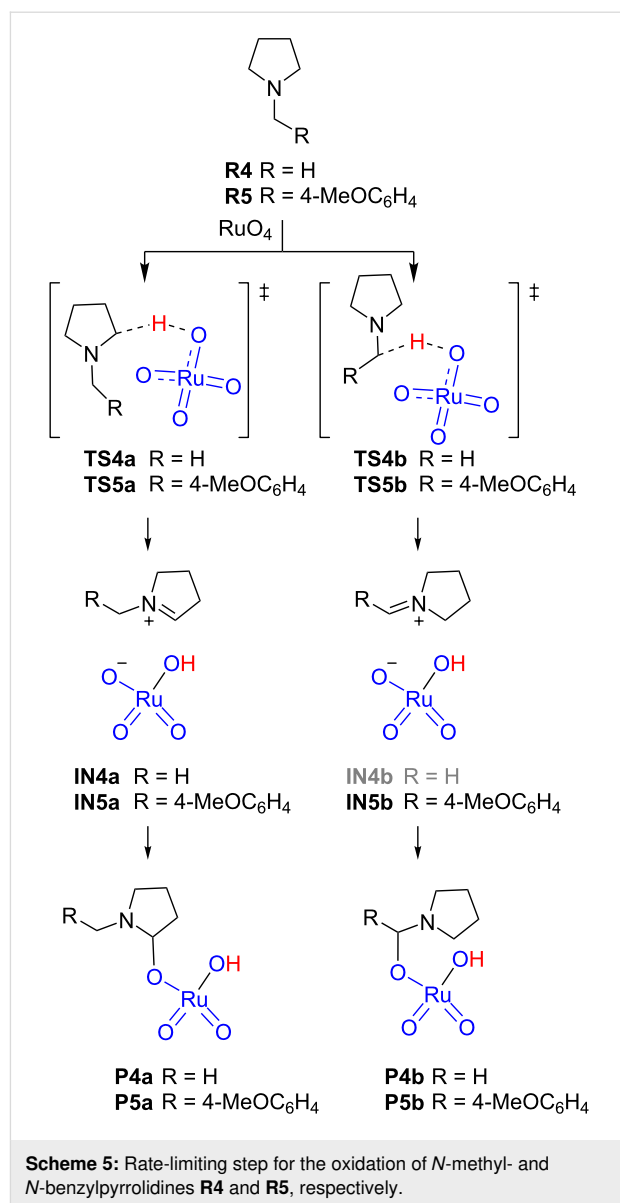
difference in favor of the *endo* oxidation was only 0.3 kcal/mol suggesting a directing effect of the *p*-methoxyphenyl group. Notably, the IRC analyses of the transition structures revealed as end points of the reactions the ion pairs **IN4,5**. Indeed, optimization of those points led to **IN4a**, **IN5a** and **IN5b** as energy minima; only **IN4b** could not be located, the optimization of which led to **P4b**. Transformation of ion pairs into the corresponding products **P4a** and **P5a,b** was found to be essentially barrierless. As expected, the ion pairs identified as minima adopt the form of an iminium ion, the most stable being **IN5b**, corresponding to that conjugated with the *p*-methoxyphenyl group, which stabilizes the positive charge. These results are in agreement with the experimental findings of Petride and co-workers, who demonstrated the existence of iminium ions as intermediates in this sort of oxidation [26].



The geometries of the transition structures showed large distances between the carbon to be oxidized and the ruthenium oxygen indicating that, in fact, they do not correspond to forming bonds (Figure 6). The largest distances correspond to the formation of *endo* iminium ions (3.61 Å and 3.63 Å for **TS4a** and **TS5a**, respectively). The shortest distance (3.24 Å) was observed for **TS4b** in agreement with the direct formation of **P4b** as mentioned above.

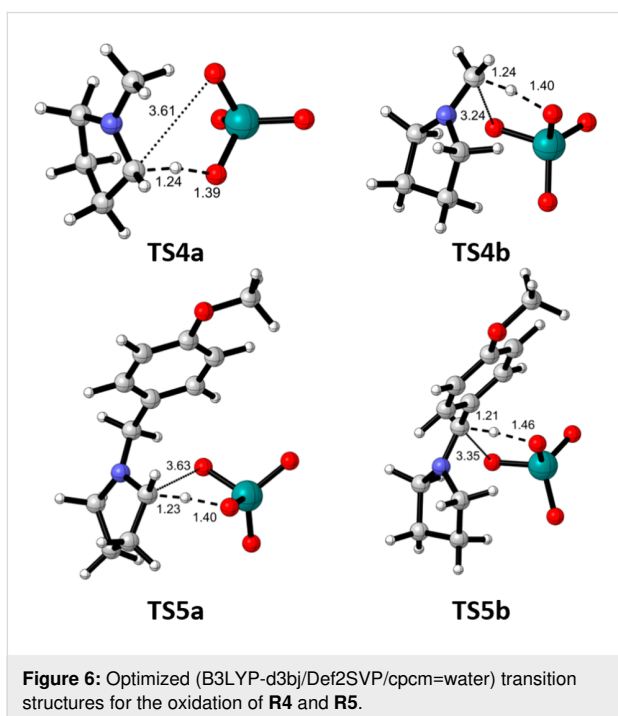
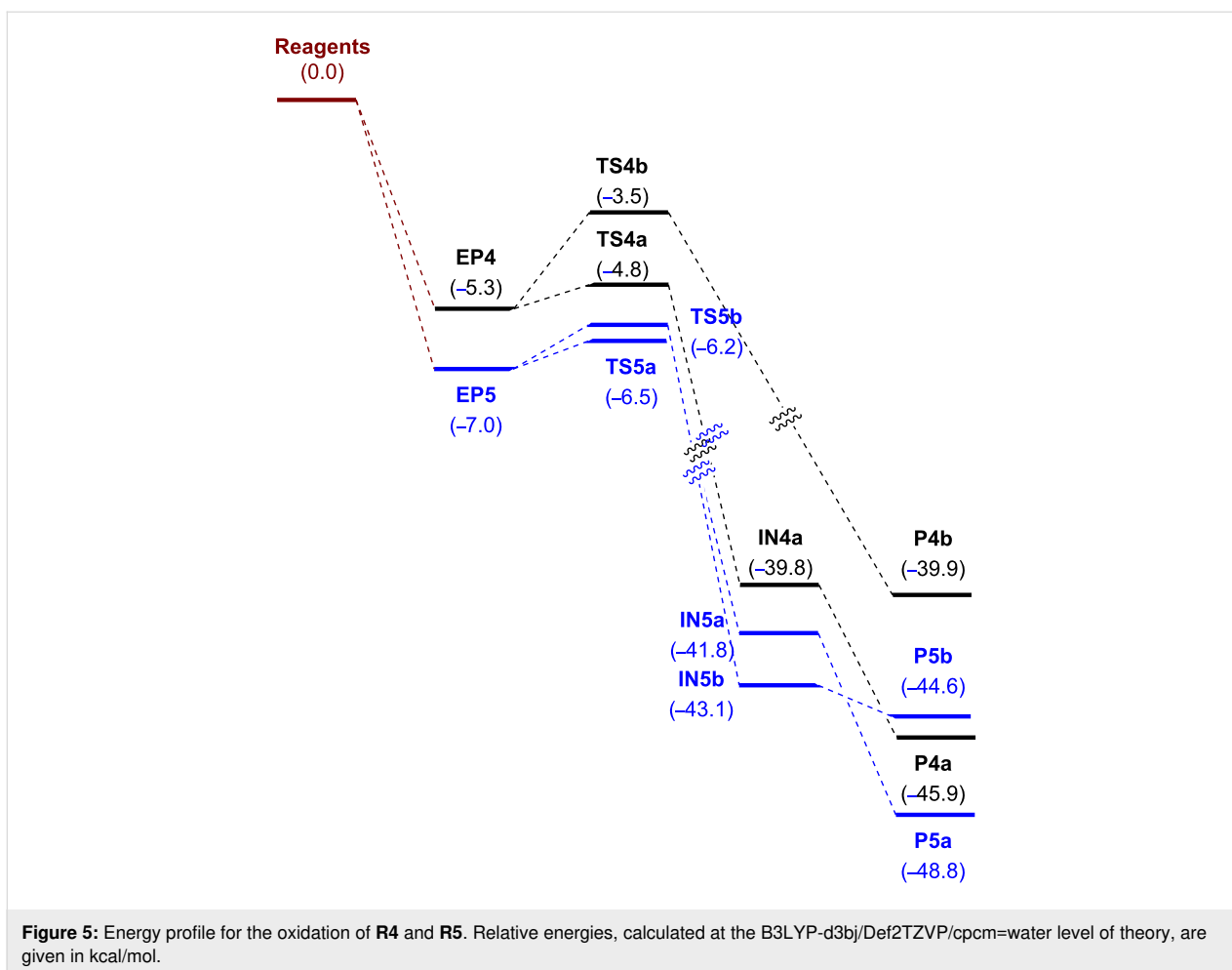
We performed the ELF analysis for the *endo* oxidation reaction of **R4** (see Supporting Information File 1) and, as expected, we only observed the H transfer corresponding to the concomitant breaking of the C–H bond and formation of the O–H bond but the resulting iminium ion was stable enough to be considered a real intermediate according to IUPAC definition of 1994, which is: “A molecular entity with a lifetime appreciably longer than a molecular vibration – corresponding to a local potential energy minimum of depth greater than  $R T$  – that is formed (directly or indirectly) from the reactants and reacts further to give (either directly or indirectly) the products of a chemical reaction” [75].

Although, according to the IUPAC definition a transient carbocation cannot be considered an intermediate (since it is required to be a local energy minimum), this transient carbocat-



ion does in fact exist, as we have demonstrated experimentally in a reaction in which the chiral information is lost as a consequence of the presence of a transient carbocation [38]. The stability of the transient carbocation can be enhanced by the presence of heteroatoms that stabilize the developing positive charge by resonance, as in the case of tetrahydrofuran and tetrahydrothiophene. Moreover, the presence of a nitrogen atom provides enough stabilization to be located as an energy minimum and to be captured experimentally [26]. Table 1 summarizes the differences observed in the studied cases.

The presence of a heteroatom contributes to lower the energy barrier of the oxidation reaction, and in the case of the pyrrolidine, it is below the reactant, demonstrating the stabilizing effect of the heteroatom in the transition structure. The asyn-

**Table 1:** Summary of results.

	barrier <sup>a</sup>	H transfer <sup>b</sup>	C–O formation <sup>b</sup>	% carbocation <sup>c</sup>
<b>R1</b>	14.6	30	49	17
<b>R2</b>	6.0	29	60	30
<b>R3</b>	7.5	17	56	40
<b>R4</b>	–3.5 <sup>d</sup>	20	– <sup>e</sup>	80

<sup>a</sup>Given in kcal/mol relative to separate reagents. <sup>b</sup>Given in % with respect to the total number of points of the IRC. <sup>c</sup>Calculated on the number of points between the H transfer and C–O bond formation with respect to the total number of points of the IRC. <sup>d</sup>The corresponding encounter pair is 8.5 kcal/mol below the reagents. <sup>e</sup>The product of the reaction is the iminium cation therefore the C–O bond is not formed.

chronicity of the reaction can be measured on the basis of the lapse between breaking of the C–H bond and formation of the C–O bond. Whereas H transfer takes places at similar moments (30% and 29% of the IRC, for the representative cases of cyclopentane (**R1**) and tetrahydrofuran (**R2**), respectively) after starting the reaction, the formation of the C–O bond takes more



time for **R2** (60% of the IRC) than for **R1** (49% of the IRC), giving more chance to the transient carbocation for the former (30% of the IRC vs 17% of the IRC for the latter).

## Conclusion

The oxidation of cyclopentane with ruthenium tetroxide is a highly polar asynchronous concerted process that during a brief lapse of time develops a transient carbocation. This result does not contradict previous calculations [25], but does point out the necessity of analyzing the full reaction coordinate to detect species that might explain some chemical behavior. Indeed, further theoretical studies on MD simulations would be needed to elucidate the lifetime of the transient carbocation [34,35]. These results demonstrate the one-step-two-stage character [42] of the ruthenium oxidations of alkanes in which H transfer and O–C bond formation take place in two separate events within the same reaction coordinate. We suggest a more adequate use of the IUPAC definition of intermediate given in 1996 [76] (*any reaction species that is neither an initial reactant nor a final product is referred to as an intermediate*) rather than that of 1994 [75], since it is in this case not strictly necessary for the transient carbocations described above to be local energy minima.

## Supporting Information

### Supporting Information File 1

Energy data, optimized geometries, full data of ELF analysis and Cartesian coordinates.

[<https://www.beilstein-journals.org/bjoc/content/supplementary/1860-5397-15-158-S1.pdf>]

## Acknowledgements

This work was supported by the Spanish Ministerio de Economía y Competitividad (MINECO) (project number CTQ2016-76155-R), by the Fondos Europeos para el Desarrollo Regional (FEDER) and the Gobierno de Aragón (Zaragoza, Spain, Groups E34-R17). The authors acknowledge the Institute of Biocomputation and Physics of Complex Systems (BIFI) at the University of Zaragoza for computer time at clusters Terminus and Memento. St. Francis-Prof. Thyagarajan Foundation (San Antonio, TX, USA) is gratefully acknowledged for a donation for software acquisition. M.-A. C. and L. L. thank Universities of Catania and Pavia for partial financial support.

## ORCID® iDs

Tomás Tejero - <https://orcid.org/0000-0003-3433-6701>

Pedro Merino - <https://orcid.org/0000-0002-2202-3460>

## References

- Murahashi, S.-I.; Komiya, N. Ruthenium-catalyzed oxidation for organic synthesis. In *Modern Oxidation Methods*, 2nd ed.; Bäckvall, J.-E., Ed.; Wiley-VCH: Weinheim, Germany, 2010; pp 241–275. doi:10.1002/9783527632039.ch7
- Arends, I. W. C. E.; Kodama, T.; Sheldon, R. A. Oxidation Using Ruthenium Catalysts. In *Ruthenium Catalysts and Fine Chemistry*; Bruneau, C.; Dixneuf, P. H., Eds.; Topics in Organometallic Chemistry, Vol. 11; Springer: Berlin, Heidelberg, 2004; pp 277–320. doi:10.1007/b94652
- Martín, V. S.; Palazón, J. M.; Rodríguez, C. M.; Nevill, C. R., Jr.; Hutchinson, D. K. Ruthenium(VIII) Oxide. *Encyclopedia of Reagents for Organic Synthesis*; John Wiley and Sons, Ltd.: Chichester, UK, 2013. doi:10.1002/047084289x.r009.pub3
- Courtney, J. L. Ruthenium Tetroxide Oxidations. In *Organic Syntheses by Oxidation with Metal Compounds*; Mijs, W. J.; de Jonge, C. R. H. I., Eds.; Plenum Press: New York, U.S.A., 1986; pp 445–467. doi:10.1007/978-1-4613-2109-5\_8
- Murahashi, S.-I.; Komiya, N. Ruthenium-Catalyzed Oxidation of Alkenes, Alcohols, Amines, Amides,  $\beta$ -Lactams, Phenols, and Hydrocarbons. In *Modern Oxidation Methods*; Bäckvall, J.-E., Ed.; Wiley-VCH: Weinheim, Germany, 2004; pp 165–191. doi:10.1002/3527603689.ch6
- Pombeiro, A. J. L.; da Silva, M. F. C. G., Eds. *Alkane Functionalization*; John Wiley & Sons, Ltd: Chichester, United Kingdom, 2019. doi:10.1002/9781119379256
- Plietker, B. *Synthesis* **2005**, 2453–2472. doi:10.1055/s-2005-872172
- Carlsen, P. H. J.; Katsuki, T.; Martin, V. S.; Sharpless, K. B. *J. Org. Chem.* **1981**, *46*, 3936–3938. doi:10.1021/jo00332a045
- Dragojlović, V.; Bajc, S.; Amblès, A.; Vitorović, D. *Org. Geochem.* **2005**, *36*, 1–12. doi:10.1016/j.orggeochem.2004.07.011
- Tanaka, K.; Yoshifuji, S.; Nitta, Y. *Chem. Pharm. Bull.* **1988**, *36*, 3125–3129. doi:10.1248/cpb.36.3125
- Kaname, M.; Yoshifuji, S.; Sashida, H. *Tetrahedron Lett.* **2008**, *49*, 2786–2788. doi:10.1016/j.tetlet.2008.02.127
- Tenaglia, A.; Terranova, E.; Waegell, B. *Tetrahedron Lett.* **1989**, *30*, 5271–5274. doi:10.1016/s0040-4039(01)93761-x
- Lee, D. G.; van den Engh, M. *Can. J. Chem.* **1972**, *50*, 2000–2009. doi:10.1139/v72-322
- Coudret, J. L.; Zöllner, S.; Ravoo, B. J.; Malara, L.; Hanisch, C.; Dörre, K.; de Meijere, A.; Waegell, B. *Tetrahedron Lett.* **1996**, *37*, 2425–2428. doi:10.1016/0040-4039(96)00325-5
- Bakke, J. M.; Lundquist, M. *Acta Chem. Scand., Ser. B* **1986**, *40*, 430–433. doi:10.3891/acta.chem.scand.40b-0430
- Tenaglia, A.; Terranova, E.; Waegell, B. *J. Chem. Soc., Chem. Commun.* **1990**, 1344–1345. doi:10.1039/c39900001344
- Bakke, J. M.; Bethell, D. *Acta Chem. Scand.* **1992**, *46*, 644–649. doi:10.3891/acta.chem.scand.46-0644
- Bakke, J. M.; Braenden, J. E. *Acta Chem. Scand.* **1991**, *45*, 418–423. doi:10.3891/acta.chem.scand.45-0418
- Tenaglia, A.; Terranova, E.; Waegell, B. *J. Org. Chem.* **1992**, *57*, 5523–5528. doi:10.1021/jo00046a040
- Coudret, J.-L.; Waegell, B. *Inorg. Chim. Acta* **1994**, *222*, 115–122. doi:10.1016/0020-1693(94)03900-3
- Bakke, J. M.; Frøhaug, A. E. *Acta Chem. Scand.* **1994**, *48*, 160–164. doi:10.3891/acta.chem.scand.48-0160
- Bakke, J. M.; Frøhaug, A. E. *J. Phys. Org. Chem.* **1996**, *9*, 507–513. doi:10.1002/(sici)1099-1395(199607)9:7<507::aid-poc811>3.0.co;2-I

23. Bakke, J. M.; Frøhaug, A. E. *Acta Chem. Scand.* **1995**, *49*, 615–622. doi:10.3891/acta.chem.scand.49-0615
24. Bakke, J. M.; Frøhaug, A. E. *J. Phys. Org. Chem.* **1996**, *9*, 310–318. doi:10.1002/(sici)1099-1395(199606)9:6<310::aid-poc790>3.0.co;2-e
25. Drees, M.; Strassner, T. *J. Org. Chem.* **2006**, *71*, 1755–1760. doi:10.1021/jo051521d
26. Petride, H.; Drăghici, C.; Florea, C.; Petride, A. *Cent. Eur. J. Chem.* **2004**, *2*, 302–322. doi:10.2478/bf02475575
27. Petride, H.; Costan, O.; Drăghici, C.; Florea, C.; Petride, A. *ARKIVOC* **2005**, No. x, 18–32.
28. Petride, H.; Drăghici, C.; Florea, C.; Petride, A. *Cent. Eur. J. Chem.* **2006**, *4*, 674–694. doi:10.2478/s11532-006-0039-8
29. Yang, Z.; Houk, K. N. *Chem. – Eur. J.* **2018**, *24*, 3916–3924. doi:10.1002/chem.201706032
30. Yang, Z.; Yu, P.; Houk, K. N. *J. Am. Chem. Soc.* **2016**, *138*, 4237–4242. doi:10.1021/jacs.6b01028
31. Xue, X.-S.; Jamieson, C. S.; Garcia-Borràs, M.; Dong, X.; Yang, Z.; Houk, K. N. *J. Am. Chem. Soc.* **2019**, *141*, 1217–1221. doi:10.1021/jacs.8b12674
32. Yu, P.; Yang, Z.; Liang, Y.; Hong, X.; Li, Y.; Houk, K. N. *J. Am. Chem. Soc.* **2016**, *138*, 8247–8252. doi:10.1021/jacs.6b04113
33. Bogle, X. S.; Singleton, D. A. *Org. Lett.* **2012**, *14*, 2528–2531. doi:10.1021/ol300817a
34. Popov, S.; Shao, B.; Bagdasarian, A. L.; Benton, T. R.; Zou, L.; Yang, Z.; Houk, K. N.; Nelson, H. M. *Science* **2018**, *361*, 381–387. doi:10.1126/science.aat5440
35. Blümel, M.; Nagasawa, S.; Blackford, K.; Hare, S. R.; Tantillo, D. J.; Sarpong, R. *J. Am. Chem. Soc.* **2018**, *140*, 9291–9298. doi:10.1021/jacs.8b05804
36. Chiacchio, M. A.; Legnani, L.; Caramella, P.; Tejero, T.; Merino, P. *Eur. J. Org. Chem.* **2017**, 1952–1960. doi:10.1002/ejoc.201700127
37. Díaz, E.; Reyes, E.; Uria, U.; Carrillo, L.; Tejero, T.; Merino, P.; Vicario, J. L. *Chem. – Eur. J.* **2018**, *24*, 8764–8768. doi:10.1002/chem.201801434
38. Ortega, A.; Manzano, R.; Uria, U.; Carrillo, L.; Reyes, E.; Tejero, T.; Merino, P.; Vicario, J. L. *Angew. Chem., Int. Ed.* **2018**, *57*, 8225–8229. doi:10.1002/anie.201804614
39. Silvi, B.; Savin, A. *Nature* **1994**, *371*, 683–686. doi:10.1038/371683a0
40. Savin, A.; Nesper, R.; Wengert, S.; Fässler, T. F. *Angew. Chem., Int. Ed. Engl.* **1997**, *36*, 1808–1832. doi:10.1002/anie.199718081
41. Merino, P.; Chiacchio, M. A.; Legnani, L.; Delso, I.; Tejero, T. *Org. Chem. Front.* **2017**, *4*, 1541–1554. doi:10.1039/c7qo00233e
42. Merino, P.; Tejero, T.; Delso, I.; Matute, R. *Org. Biomol. Chem.* **2017**, *15*, 3364–3375. doi:10.1039/c7ob00429j
43. Chiacchio, M.-A.; Legnani, L.; Caramella, P.; Tejero, T.; Merino, P. *Tetrahedron* **2018**, *74*, 5627–5634. doi:10.1016/j.tet.2018.07.056
44. Spitzer, U. A.; Lee, D. G. *J. Org. Chem.* **1975**, *40*, 2539–2540. doi:10.1021/jo00905a029
45. Lee, D. G.; van den Engh, M. *Can. J. Chem.* **1972**, *50*, 3129–3134. doi:10.1139/v72-501
46. Tangari, N.; Tortorella, V. *J. Chem. Soc., Chem. Commun.* **1975**, 71b–72. doi:10.1039/c3975000071b
47. *Gaussian*; Gaussian Inc.: Wallingford, CT, 2009.
48. Becke, A. D. *J. Chem. Phys.* **1993**, *98*, 5648–5652. doi:10.1063/1.464913
49. Lee, C.; Yang, W.; Parr, R. G. *Phys. Rev. B* **1988**, *37*, 785–789. doi:10.1103/physrevb.37.785
50. Grimme, S.; Ehrlich, S.; Goerigk, L. *J. Comput. Chem.* **2011**, *32*, 1456–1465. doi:10.1002/jcc.21759
51. Grimme, S.; Antony, J.; Ehrlich, S.; Krieg, H. *J. Chem. Phys.* **2010**, *132*, 154104. doi:10.1063/1.3382344
52. Weigend, F. *Phys. Chem. Chem. Phys.* **2006**, *8*, 1057–1065. doi:10.1039/b515623h
53. Weigend, F.; Ahlrichs, R. *Phys. Chem. Chem. Phys.* **2005**, *7*, 3297–3305. doi:10.1039/b508541a
54. Barone, V.; Cossi, M. *J. Phys. Chem. A* **1998**, *102*, 1995–2001. doi:10.1021/jp9716997
55. Cossi, M.; Rega, N.; Scalmani, G.; Barone, V. *J. Comput. Chem.* **2003**, *24*, 669–681. doi:10.1002/jcc.10189
56. Schlegel, H. B. Geometry optimization on potential energy surfaces. In *Modern Electronic Structure Theory, Part I*; Yarkony, D. R., Ed.; World Scientific Publishing: Singapore, 1995; pp 459–500. doi:10.1142/9789812832108\_0008
57. Fukui, K. *J. Phys. Chem.* **1970**, *74*, 4161–4163. doi:10.1021/j100717a029
58. Hratchian, H. P.; Schlegel, H. B. *J. Phys. Chem. A* **2002**, *106*, 165–169. doi:10.1021/jp012125b
59. Tanaka, R.; Yamashita, M.; Chung, L. W.; Morokuma, K.; Nozaki, K. *Organometallics* **2011**, *30*, 6742–6750. doi:10.1021/om2010172
60. Savin, A.; Becke, A. D.; Flad, J.; Nesper, R.; Preuss, H.; von Schnering, H. G. *Angew. Chem., Int. Ed. Engl.* **1991**, *30*, 409–412. doi:10.1002/anie.199104091
61. Savin, A.; Nesper, R.; Wengert, S.; Fässler, T. F. *Angew. Chem., Int. Ed. Engl.* **1997**, *36*, 1808–1832. doi:10.1002/anie.199718081
62. Savin, A.; Silvi, B.; Colonna, F. *Can. J. Chem.* **1996**, *74*, 1088–1096. doi:10.1139/v96-122
63. Silvi, B. *J. Mol. Struct.* **2002**, *614*, 3–10. doi:10.1016/s0022-2860(02)00231-4
64. Llusar, R.; Beltrán, A.; Andrés, J.; Noury, S.; Silvi, B. *J. Comput. Chem.* **1999**, *20*, 1517–1526. doi:10.1002/(sici)1096-987x(19991115)20:14<1517::aid-jcc4>3.0.co;2-#
65. Silvi, B.; Fourré, I.; Alikhani, M. E. *Monatsh. Chem.* **2005**, *136*, 855–879. doi:10.1007/s00706-005-0297-8
66. Andrés, J.; Berski, S.; Feliz, M.; Llusar, R.; Sensato, F.; Silvi, B. *C. R. Chim.* **2005**, *8*, 1400–1412. doi:10.1016/j.crci.2004.12.014
67. Noury, S.; Krokidis, X.; Fuster, F.; Silvi, B. *Comput. Chem. (Oxford, U. K.)* **1999**, *23*, 597–604. doi:10.1016/s0097-8485(99)00039-x
68. *CYLview*, 1.0b; Legault, C. Y.; Université de Sherbrooke, 2009. <http://www.cylview.org>.
69. Domingo, L. R.; Arno, M.; Saez, J. A. *J. Org. Chem.* **2009**, *74*, 5934–5940. doi:10.1021/jo900889q
70. Roca-López, D.; Polo, V.; Tejero, T.; Merino, P. *J. Org. Chem.* **2015**, *80*, 4076–4083. doi:10.1021/acs.joc.5b00413
71. Roca-López, D.; Polo, V.; Tejero, T.; Merino, P. *Eur. J. Org. Chem.* **2015**, 4143–4152. doi:10.1002/ejoc.201500447
72. Becke, A. D.; Edgecombe, K. E. *J. Chem. Phys.* **1990**, *92*, 5397–5403. doi:10.1063/1.458517
73. Andres, J.; Berski, S.; Domingo, L. R.; Polo, V.; Silvi, B. *Curr. Org. Chem.* **2011**, *15*, 3566–3575. doi:10.2174/138527211797636156
74. Savin, A. *J. Chem. Sci.* **2005**, *117*, 473–475. doi:10.1007/bf02708351
75. Muller, P. *Pure Appl. Chem.* **1994**, *66*, 1077–1184. doi:10.1351/pac199466051077
76. Laidler, K. J. *Pure Appl. Chem.* **1996**, *68*, 149–192. doi:10.1351/pac199668010149

## License and Terms

This is an Open Access article under the terms of the Creative Commons Attribution License (<http://creativecommons.org/licenses/by/4.0>). Please note that the reuse, redistribution and reproduction in particular requires that the authors and source are credited.

The license is subject to the *Beilstein Journal of Organic Chemistry* terms and conditions: (<https://www.beilstein-journals.org/bjoc>)

The definitive version of this article is the electronic one which can be found at:  
[doi:10.3762/bjoc.15.158](https://doi.org/10.3762/bjoc.15.158)